NJC

PAPER

View Article Online
View Journal | View Issue

Published on 11 August 2014. Downloaded by University of Prince Edward Island on 27/10/2014 08:59:50.

Cite this: *New J. Chem.*, 2014, **38**, 5087

Triazine–pyrimidine based molecular hybrids: synthesis, docking studies and evaluation of antimalarial activity†

Deepak Kumar,[a] Shabana I. Khan,[b] Prija Ponnan[a] and Diwan S. Rawat*[a]

Received (in Montpellier, France) 13th June 2014,
Accepted 11th August 2014

DOI: 10.1039/c4nj00978a

www.rsc.org/njc

A series of novel triazine–pyrimidine hybrids have been synthesized and evaluated for their *in vitro* antimalarial activity. Some of the compounds showed promising antimalarial activity against both CQ-sensitive and CQ-resistant strains at micromolar level with a high selectivity index. All the compounds displayed better activity (IC_{50} = 1.32–10.70 μM) than the standard drug pyrimethamine (>19 μM) against the chloroquine-resistant strain W2. All the tested compounds were nontoxic against mammalian cell lines. Further, docking studies of the most active compounds were performed on both wild type and quadruple mutant (N51I, C59R, S108N, I164L) PfDHFR-TS using Glide to analyse the interaction of the compounds with the binding site of the protein. The binding poses of compounds **14** and **19**, having a high Glide XP score and the lowest Glide energies, show an efficient binding pattern similar to that of the DHFR substrate (dihydrofolate) in the wild type and mutant DHFR active site. The analysis of the pharmacokinetic properties of the most active compounds using ADMET prediction attests to the possibility of developing compound **14** as a potent antimalarial lead.

Introduction

Malaria is the third most infectious disease after tuberculosis and HIV/AIDS, and affects over 100 countries in Africa, Asia and South America.[1] Despite intensive efforts towards its eradication in the early 1960s, malaria remains a major public health problem to date. According to the World Health Organization (WHO) nearly 300–500 million people throughout the world become infected with malaria every year. The mortality rate is estimated to be around 1.1 million deaths per year, mostly children under the age of five. Eighty percent of malaria cases worldwide occur in Africa; two thirds of the remaining cases are found in six countries, of which India is one. There are four major species of the malaria parasite, of which *Plasmodium falciparum* causes the most virulent forms of malaria and is responsible for more than 95% of malaria-related deaths. Due to the unavailability of effective vaccines, chemotherapy remains the only option for the treatment of malaria. After the discovery of quinine in the late 1600s, a huge number of potent antimalarial agents such as chloroquine, amodiaquine, primaquine, pamaquine, mefloquine and related compounds were developed. Chloroquine (CQ) has been the mainstay of malaria therapy for decades because of its efficacy, safety and low cost, until the emergence and spread of CQ-resistance. Pyrimethamine-sulfadoxine (Fansidar) was one of the best therapeutic options after CQ, but was rendered ineffective in most malaria-endemic regions due to the spread of resistance. Currently, natural endoperoxide artemisinin and its semi-synthetic derivatives (artemether, arteether and artesunate) are the most potent and fast-acting antimalarials effective against resistant strains of *P. falciparum*. In order to combat the resistance problem, combination therapy has been introduced by the WHO, in which artemisinin and its analogue in combination with 4-aminoquinoline antimalarials are used to treat malaria. Although artemisinin combination therapy (ACT) is well-tolerated and is nearly 95% effective in treating malaria, its use is limited in some regions due to some serious issues such as the higher cost of treatment and safety during pregnancy.[2–7] In addition, resistance to artemisinin derivatives has also been reported in Southeast Asian countries and may continue to increase, subsequently making malaria chemotherapy more complicated.[5–8]

Dihydrofolate reductase (DHFR) is one of the more well-defined and explored targets in malarial chemotherapy. Pyrimethamine and cycloguanil (Fig. 1) are potent DHFR inhibitors and are clinically used for the treatment of *P. falciparum* malaria.[9,10] Unfortunately, point mutations at certain amino acid residues in the surroundings of the active site of *P. falciparum* DHFR have resulted in resistance, compromising the clinical effectiveness of

[a] *Department of Chemistry, University of Delhi, Delhi-110007, India. E-mail: dsrawat@chemistry.du.ac.in; Fax: +91-11-27667501; Tel: +91-11-27667465*
[b] *National Centre for Natural Products Research, University of Mississippi, MS-38677, USA*

† Electronic supplementary information (ESI) available. See DOI: 10.1039/c4nj00978a

Published on 11 August 2014. Downloaded by University of Prince Edward Island on 27/10/2014 08:59:50.

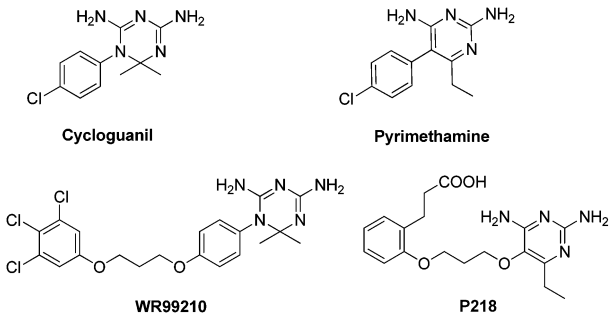

Fig. 1 DHFR inhibitor-based antimalarial drugs.

these drugs.[11–13] Despite this, the folate pathway remains a good target for malarial chemotherapy because the enzyme is limited in its mutational capability, owing to the loss in enzyme function. WR99210 (Fig. 1), having a flexible linker, is found to be effective at nanomolar concentration even against the strains that are highly resistant to other DHFR inhibitors. It is believed that the exceptionally high activity of WR99210 is due to its highly flexible nature, which helps to bind it into the active site of the target.[14] Unfortunately, WR99210 exhibits unacceptable gastrointestinal (GI) intolerance. Recently, a new DHFR inhibitor, P218 (Fig. 1), has been developed by BIOTEC pharmaceuticals.[15,16] It inhibits blood stage growth of drug-resistant malarial parasites with an IC_{50} value of 6 nM. It is also the most active antifolate agent against the liver stage of *P. yoelii* ($IC_{50} < 10$ nM).[17]

Apart from this, a large number of structurally similar compounds such as triazine[18–20] and pyrimidine derivatives[21–23] have been synthesized, and some of these compounds have shown very potent antimalarial activity against both CQ-sensitive and CQ-resistant strains. Cycloguanil and pyrimethamine represent the triazine and pyrimidine classes of compounds, respectively. To combat the increasing resistance problem, there is an urgent need to develop a potent, safe and cost-effective antimalarial agent. As part of our ongoing malaria research programme,[24–30] we became interested in joining triazine and pyrimidine moieties together in a single molecule, using a flexible linker to provide the molecule with enough flexibility so that, like WR99210, it can easily fit into the binding pocket of the target, and so may have a better antimalarial activity profile as a result. To the best of our knowledge, this is the first report of covalent hybrids having both triazine and pyrimidine pharmacophores. All the synthesized compounds were characterized by various spectroscopic techniques.

Chemistry

The triazine–pyrimidine hybrids **14–31** (Fig. 2) were synthesized as shown in three different Schemes (1–3). Firstly, 2,4-dichloropyrimidine (**1**) was treated with different secondary amines in the presence of triethylamine in THF at 0 °C to RT to give compounds **2–4** in high yield, with small amounts of the regioisomer (Scheme 1).[31] 2,4,6-Trichloro-1,3,5-triazine shows temperature-dependent nucleophilic substitution reactions, with the first chlorine being replaceable at 0 °C, the second chlorine at room temperature and the third at higher temperature.

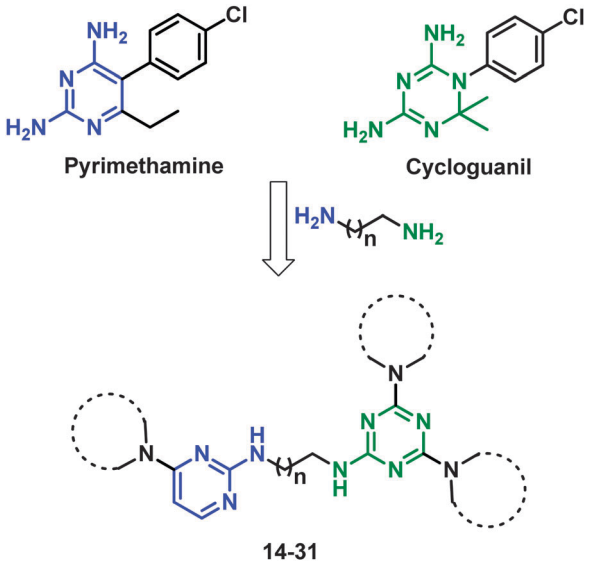

Fig. 2 Design strategy for the synthesis of novel triazine–pyrimidine hybrids.

The disubstituted products **6** and **7** were obtained by the reaction of triazine (**5**) with two equivalents of either morpholine or diethylamine, respectively, at 0 °C to RT (<30 °C) in the presence of K_2CO_3 using THF as the solvent (Scheme 2).[32,33] Thereafter, the resulting disubstituted triazines were reacted, by substitution of the third chlorine, with various alkyl diamines to give trisubstituted triazines (**8–13**) with a free terminal NH_2 group (Scheme 2).[34] This reaction was carried out under reflux conditions in THF using K_2CO_3 as a base. Finally, compounds **2–4** and **8–13**, synthesized as shown in Schemes 1 and 2, were coupled together in the presence of K_2CO_3, using NMP as a solvent and under reflux conditions, to give the desired triazine–pyrimidine hybrid molecules **14–31** (Scheme 3). All the compounds were purified by column chromatography using MeOH–$CHCl_3$ as eluent and characterized by various spectroscopic techniques.

Biological activity

In vitro antimalarial activity

The antimalarial activity was determined by measuring plasmodial LDH activity as described in the literature.[35] A suspension of red blood cells infected with the D6 or W2 strain of *P. falciparum* (200 μL, with 2% parasitemia and 2% hematocrit in RPMI 1640 medium supplemented with 10% human serum and 60 μg mL^{-1} amikacin) was added to the wells of a 96-well plate containing 10 μL of serially diluted test samples. The plate was flushed with a gas mixture of 90% N_2, 5% O_2, and 5% CO_2 and incubated at 37 °C for 72 h in a modular incubation chamber (Billups-Rothenberg, CA). Parasitic LDH activity was determined according to the procedure of Makler and Hinrichs.[36] 20 μL of the incubation mixture was mixed with 100 μL of the Malstat™ reagent (Flow Inc., Portland, OR) and incubated at room temperature for 30 min. Twenty microliters of a 1 : 1 mixture of NBT/PES (Sigma, St. Louis, MO) was then added and the plate was further incubated in the dark for 1 h.

 This journal is © The Royal Society of Chemistry and the Centre National de la Recherche Scientifique 2014

Published on 11 August 2014. Downloaded by University of Prince Edward Island on 27/10/2014 08:59:50.

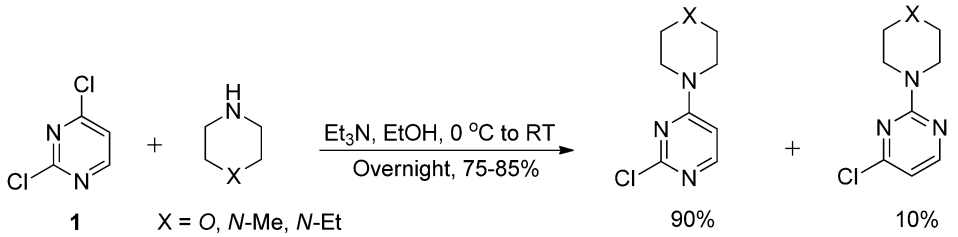

Scheme 1

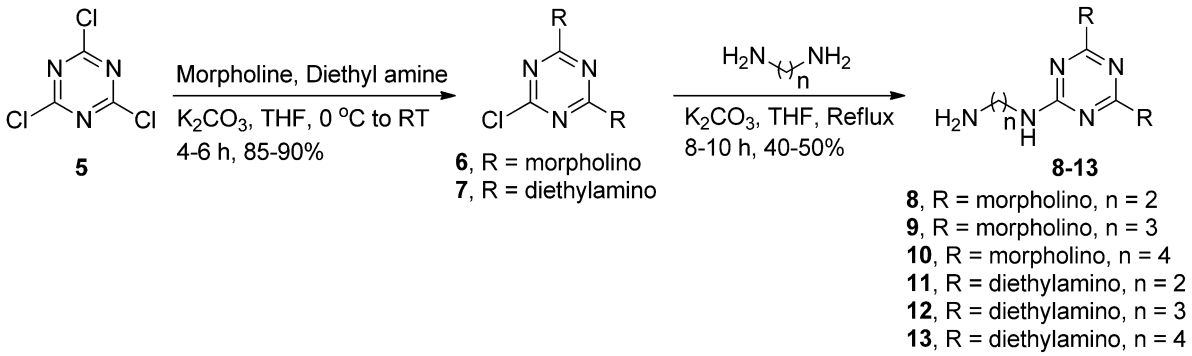

Scheme 2

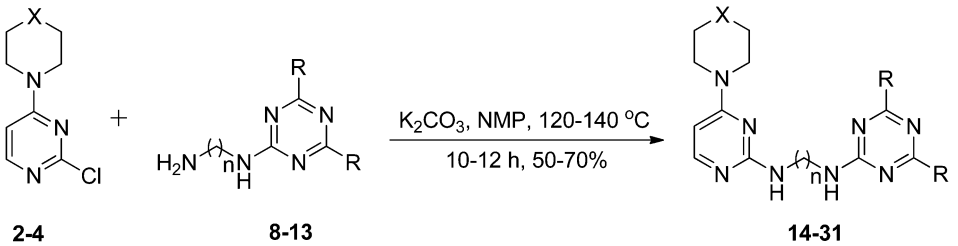

14, R = morpholino, X = O, n = 2
15, R = morpholino, X = O, n = 3
16, R = morpholino, X = O, n = 4
17, R = morpholino, X = *N*-Me, n = 2
18, R = morpholino, X = *N*-Me, n = 3
19, R = morpholino, X = *N*-Me, n = 4
20, R = morpholino, X = *N*-Et, n = 2
21, R = morpholino, X = *N*-Et, n = 3
22, R = morpholino, X = *N*-Et, n = 4
23, R = diethylamino, X = O, n = 2
24, R = diethylamino, X = O, n = 3
25, R = diethylamino, X = O, n = 4
26, R = diethylamino, X = *N*-Me, n = 2
27, R = diethylamino, X = *N*-Me, n = 3
28, R = diethylamino, X = *N*-Me, n = 4
29, R = diethylamino, X = *N*-Et, n = 2
30, R = diethylamino, X = *N*-Et, n = 3
31, R = diethylamino, X = *N*-Et, n = 4

Scheme 3

The reaction was then stopped by the addition of 100 μL of a 5% acetic acid solution. The plate was read at 650 nm. Chloroquine and pyrimethamine were included in each assay as antimalarial drug controls. IC_{50} values were computed from the dose–response curves. To determine the selectivity index of the antimalarial activity of the compounds, *in vitro* cytotoxicity of these compounds against mammalian cells was also determined. The assay was performed in 96-well tissue culture-treated plates as described earlier.[37] VERO cells (monkey kidney fibroblasts) were seeded into the wells of 96-well plates at a density of 25 000 cells per well and incubated for 24 h. Samples at different concentrations were added and the plates were again incubated for 48 h. The number of viable cells was determined by Neutral Red assay. The IC_{50} values were obtained from dose–response curves.

Docking studies

Antifolates act by inhibiting the dihydrofolate reductase activity of *Plasmodium falciparum* bifunctional enzyme dihydrofolate

Published on 11 August 2014. Downloaded by University of Prince Edward Island on 27/10/2014 08:59:50.

reductase-thymidylate synthase (PfDHFR-TS). The four point mutations in codons 51, 59, 108, and 164 (N51I, C59R, S108N, and I164L) have been found in the DHFR domain of the PfDHFR-TS gene from the clinical isolates of dihydrofolate-resistant parasite.[38] In the present work we have studied the binding pattern and ADMET properties of novel triazine–pyrimidine hybrids with PfDHFR-TS. The 2D structures of all the compounds were generated using ChemBioDraw Ultra 12.0 (www.cambridgesoft.com) and the Ligprep module in Schrödinger was used to generate energy-minimized 3D structures. Partial atomic charges were computed using the OPLS_2005 force field. The correct Lewis structure, tautomers and ionization states (pH 7.0 ± 2.0) for each of these ligands were generated and optimized with default settings (Ligprep 2.5, Schrödinger, LLC, New York, NY, 2012). The 3D crystal structures of wild type PfDHFR-TS (PDB ID: 3QGT; resolution 2.30 Å) and quadruple mutant (N51I + C59R + S108N + I164L) PfDHFR-TS (PDB ID: 3QG2; resolution: 2.30 Å) were retrieved from the protein data bank (www.rcsb.org). The proteins were prepared for docking using the Protein Preparation Wizard (Maestro 10.0 Schrödinger, LLC, New York, NY, 2012). Water molecules within 5 Å of the protein structures were considered. Bond order and formal charges were assigned and hydrogen atoms were added to the crystal structure. To further refine the structure, an OPLS-2005 force field parameter was used to alleviate steric clashes and the minimization was terminated when RMSD reached a maximum cutoff value of 0.30 Å.

The location of co-crystallized ligand pyrimethamine in both wild and mutant protein structures was used to choose the center and size of the receptor grid, which was generated using Glide 5.8 (Schrödinger, LLC, New York, NY, 2012) with default settings for all parameters. The grid size was chosen to be sufficiently large so as to include all active site residues involved in substrate binding. The cofactor NADH in the PfDHFR-TS wild and mutant structures was also considered as part of the receptor protein. All ligand conformers were docked to each of the receptor grid files (PfDHFR-TS wild and mutant structures) using Glide extra precision (XP) mode. Default settings were used for the refinement and scoring.

In silico ADMET prediction

The pharmacokinetic profile of compounds showing good antimalarial activity was predicted using the QikProp v3.5 program (Schrödinger, Inc., New York, NY, 2012). All the compounds were prepared in neutralized form for the calculation of pharmacokinetic properties by QikProp using Schrödinger's Maestro Build module and LigPrep, saved in SD format. The QikProp program utilizes the method of Jorgensen[39] to compute pharmacokinetic properties and descriptors such as the octanol/water partitioning coefficient, aqueous solubility, brain/blood partition coefficient, intestinal wall permeability and plasma protein binding.

Results and discussion

The triazine–pyrimidine hybrids were evaluated for their *in vitro* antimalarial activity against both CQ-sensitive (D6 clone) and CQ-resistant (W2 clone) strains of *P. falciparum* using chloroquine and pyrimethamine as standard drugs. Cytotoxicity was determined against VERO cells (Table 1). All compounds except for **16**, **17** and **23** exhibited promising antimalarial activity with IC_{50} values of <5 μM against the chloroquine-sensitive strain (D6). Four compounds (**14**, **27**, **28** and **30**) displayed potent antimalarial activity with IC_{50} values ranging from 1.18 μM to 1.57 μM against the CQ-sensitive strain and a high selectivity index, while other compounds showed moderate to good antimalarial activity. None of these compounds showed any cytotoxicity towards mammalian kidney fibroblast (VERO cells). In the case of the CQ-resistant strain, the compounds also showed significant activity (IC_{50} <10 μM). It is interesting to note that all the compounds were found to be more active than the standard drug pyrimethamine against the chloroquine-resistant strain (W2). Compound **14** showed potent activity against both the strains.

Table 1 *In vitro* antimalarial activity and cytotoxicity of triazine–pyrimidine hybrids[a]

Compound	*P. falciparum* (D6 clone)		*P. falciparum* (W2 clone)		Cytotoxicity (VERO cells)
	IC_{50} (μM)	SI	IC_{50} (μM)	SI	IC_{50} (μM)
14	1.18	>8.53	1.32	>7.62	>10.07
15	4.41	>2.21	7.48	>1.30	>9.78
16	6.21	>1.52	8.83	>1.07	>9.50
17	>9.80	1.00	>9.80	1.00	>9.80
18	3.88	>2.45	4.60	>2.06	>9.52
19	2.15	>4.30	2.62	>3.53	>9.26
20	4.54	>2.09	5.52	>1.72	>9.52
21	3.67	>2.52	5.86	>1.58	>9.26
22	4.32	>2.08	4.60	>1.96	>9.02
23	10.29	>1.03	>10.70	1.00	>10.70
24	3.05	>3.40	7.39	>1.40	>10.37
25	2.22	>4.53	9.98	>1.00	>10.07
26	3.46	>3.00	4.86	>2.13	>10.40
27	1.28	>7.88	3.07	>3.28	>10.09
28	1.54	>6.36	4.04	>2.42	>9.80
29	4.85	>2.08	7.96	>1.26	>10.09
30	1.57	>6.24	4.79	>2.04	>9.80
31	2.50	>3.80	4.70	>2.02	>9.52
CQ	0.04	>1500	0.39	>150	>60
Pyr	0.01	1820	[b]	—	18.2

[a] IC_{50}: the concentration that causes 50% growth inhibition; SI: selectivity index (IC_{50} for cytotoxicity to VERO cells/IC_{50} for antimalarial activity). [b] Not active up to 19 μM.

The activity profile of these compounds against the CQ-sensitive strain of *P. falciparum* clearly indicates that the compounds having *N*-methyl or *N*-ethyl groups at the pyrimidine nucleus were found to be more active than the compounds having a morpholine ring (**15** *vs.* **18** and **21**, **16** *vs.* **19**, **22**). Similarly, compounds having a diethyl amino group at the triazine nucleus (**24–31**) were found to be more active than the respective compounds having a morpholine ring at the triazine nucleus (**15–22**), with the exception of compounds **14** and **23** where compound **14** was more active than compound **23**. Compounds having a diethyl group at the triazine nucleus and *N*-methyl or *N*-ethyl groups at the pyrimidine nucleus (**27**, **28**, **30** and **31**) were more potent than other compounds. Although in the case of the CQ-resistant strain no uniform pattern was observed, compounds with a long carbon chain between the triazine and pyrimidine ring showed better activity

 This journal is © The Royal Society of Chemistry and the Centre National de la Recherche Scientifique 2014

Published on 11 August 2014. Downloaded by University of Prince Edward Island on 27/10/2014 08:59:50.

Table 2 Glide docking scores (kcal mol^{-1}) and docking energies of the most active molecules along with the reference compounds (pyrimethamine, cycloguanil and WR99210) and dihydrofolate in the binding site of wild and mutant PfDHFR-TS

	Docking results with wild PfDHFR				Docking results with mutant PfDHFR				
Compounds	XP G score	van der Waals energy	Coulomb energy	Glide energy	XP H-bond	XP G score	van der Waals energy	Coulomb energy	Glide energy
14	−6.25	−51.18	−6.65	−57.84	−1.99	−6.50	−41.17	−9.5	−57.11
19	−4.71	−46.48	−6.08	−46.31	−1.04	−6.1	−29.81	−4.98	−39.09
25	−2.13	−21.04	−1.98	−14.76	−0.12	−2.98	−23.51	−3.42	−28.03
27	−3.04	−28.90	−3.26	−28.78	−0.23	−3.92	−28.08	−3.14	−37.65
28	−3.22	−23.76	−2.32	−21.43	−0.26	−3.17	−23.74	−3.26	−29.73
30	−2.75	−32.65	−2.09	−26.54	−0.17	−3.36	−29.54	−3.65	−32.54
31	−1.98	−22.45	−0.97	−14.52	−0.18	−2.05	−21.62	−3.05	−23.65
Dihydrofolate	−9.33	−52.14	−14.19	−64.84	−3.10	−11.00	−43.68	−17.61	−61.30
Pyrimethamine	−9.04	−31.70	−15.51	−44.91	−2.64	−9.39	−33.65	−12.06	−43.55
Cycloguanil	−8.94	−30.12	−10.74	−38.55	−2.86	−8.95	−34.30	−8.60	−46.6
WR99210	−4.84	−51.18	−6.91	−37.03	−2.09	−5.48	−27.37	−8.07	−34.30

than compounds having a short carbon chain. Amongst all compounds, **14** was found to be the most potent compound with IC_{50} values of 1.18 μM against the chloroquine-sensitive strain (D6) and 1.32 μM against the chloroquine-resistant strain (W2).

Molecular docking studies of the most active compounds (**14**, **19**, **25**, **27**, **28**, **30** and **31**) were performed in the binding pocket of both the wild type PfDHFR-TS (PDB ID: 3QGT) and quadruple mutant PfDHFR-TS (N51I, C59R, S108N, I164L, PDB ID: 3QG2) structures. The results of the docking studies and the docked conformations of the best scoring ligands (**14** and **19**) in the active site of wild and mutant PfDHFR-TS are summarized in Table 2 and Fig. 3 and 4. These docking results clearly indicate that the most active compounds in the study exhibited significant binding affinities towards the wild (Glide energy range −57.84 kcal mol^{-1} to −14.52 kcal mol^{-1}) and quadruple mutant (Glide energy range −57.11 kcal mol^{-1} to −23.65 kcal mol^{-1}) PfDHFR-TS structures, and the energy ranges are comparable to the standard PfDHFR inhibitors (pyrimethamine, cycloguanil and WR99210) and the native DHFR substrate, dihydrofolate (Table 2).

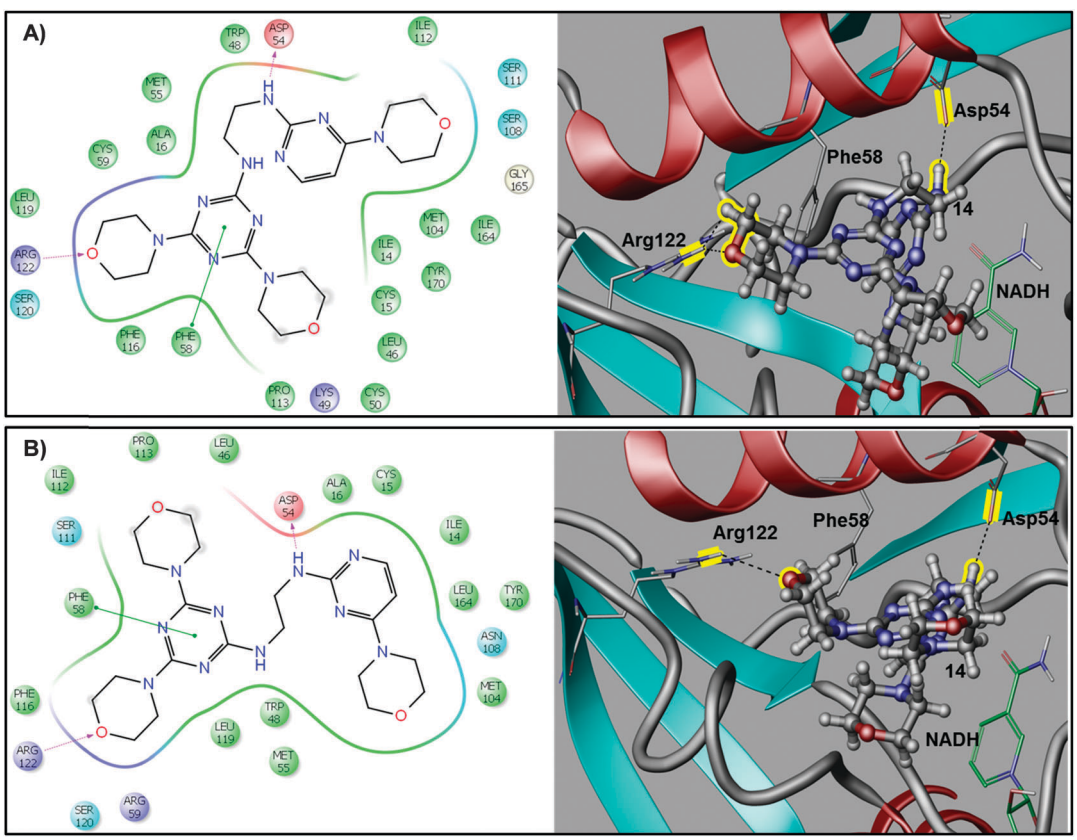

Fig. 3 2D and 3D docking poses showing the interactions of compound **14** in the binding site of (A) wild (PDB ID: 3QGT) and (B) mutant PfDHFR-TS (PDB ID: 3QG2).

Published on 11 August 2014. Downloaded by University of Prince Edward Island on 27/10/2014 08:59:50.

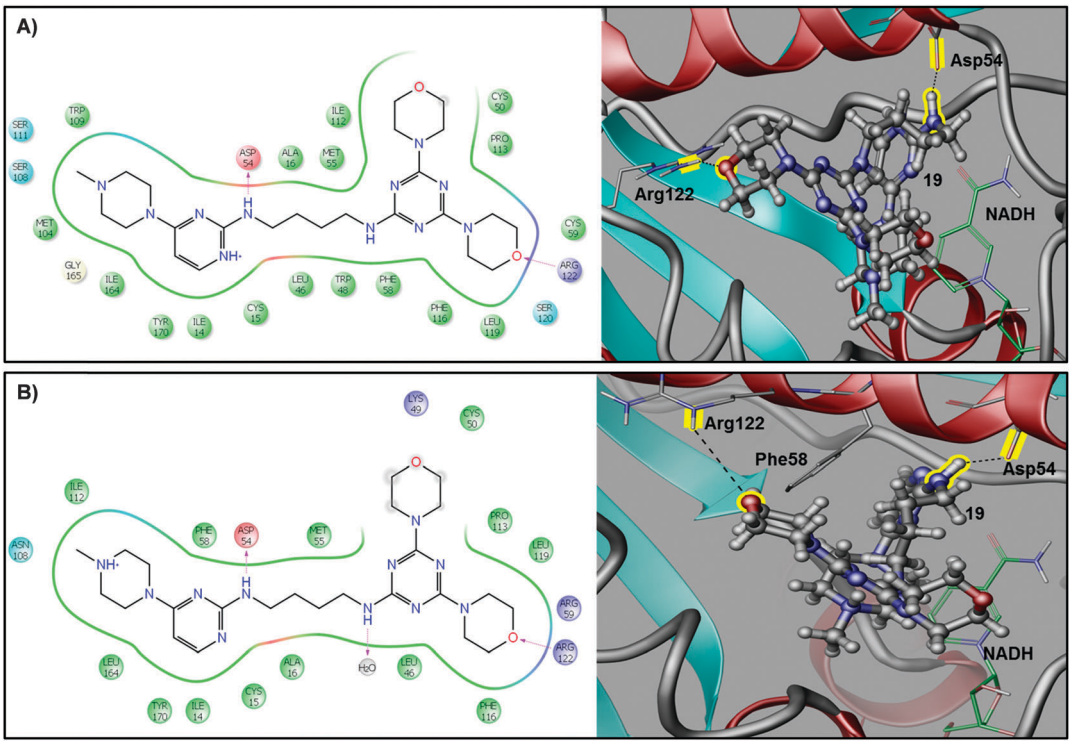

Fig. 4 2D and 3D docking poses showing the interactions of compound **19** in the binding site of (A) wild (PDB ID: 3QGT) and (B) mutant PfDHFR-TS (PDB ID: 3QG2).

Fig. 3 and 4 illustrate the predicted binding poses for compounds **14** and **19**, showing hydrogen bonding along with π–π interactions and van der Waals interactions, with the expected binding pattern as observed for PfDHFR inhibitors and dihydrofolate in the wild type and mutant PfDHFR protein.[24] Compound **14**, showing the lowest binding energy (−57.84 kcal mol^{-1}) and a considerably high Glide XP score (−6.50 kcal mol^{-1}) for mutant PfDHFR, binds deep in the DHFR binding site, forming a hydrogen bond between the linker NH group of **14** and the carboxylate oxygen side chain of Asp54 in both wild type and mutant PfDHFR. The morpholine rings attached to the triazine moiety of the compound **14** lie in the opposite end of the active site when bound to mutant PfDHFR, forming a charge-mediated hydrogen bond between one of the morpholine ring oxygen heteroatoms and the side chain nitrogen atom of Arg122 (Fig. 3B). Further, a π–π interaction between the aromatic ring of Phe58 and the triazine ring of the compound was observed. A similar interaction pattern was observed for compound **14** (Glide energy: −57.84 kcal mol^{-1}) in the binding site of wild type PfDHFR (Fig. 3A). Compound **19** was predicted to have a low binding energy and high Glide score in wild type and mutant PfDHFR (Table 2), with a H-bonding pattern between the linker NH group of the compound and the carboxylate oxygen side chain of Asp54 and a charge-mediated H-bond between the morpholine oxygen and the Arg122 side chain (Fig. 4B).

The influence of quadruple mutations (N51I, C59R, S108N, I164L) in DHFR is attributed to the movement in the active site residues, and interferes in the inhibitor binding. The active site residue Asp54, forming a H-bond with test compounds **14** and **19**, has been reported to be crucial for inhibitor and substrate (dihydrofolate) binding and lies in the proximity of residues 51 and 59. C59R mutation does not cause any significant changes in the protein structure and causes no close contacts with the inhibitors. N51I causes movement in the main chain atoms of residues 48–51. Moreover, the function of the residue Asp54 is preserved in the mutant protein and is not affected by the two proximal mutations N51I and C59R.[40] Further, I164L mutation causes shifts in the residues 164–167 and affects the active site gap, causing steric interactions between Phe58 and small inhibitors such as pyrimethamine and cycloguanil.[40] Also, the *p*-chlorophenyl moiety in pyrimethamine and cycloguanil causes steric interference with the side chain of Asn108 in the active site modified by the first mutation S108N. In contrast, WR99210, endowed with a long and flexible side chain, could avoid such steric interactions, leading to effective binding with the mutant protein. The test compounds **14** and **19**, having a flexible linker similar to WR99210, form π–π interactions with Phe58, thus avoiding a steric clash with the aromatic side chain of Phe58. Furthermore, the oxygen atom in the morpholine side chain linked to the triazine nucleus of compounds **14** and **19** forms a H-bonding interaction with evolutionarily conserved Arg122. Such a charge-mediated interaction of Arg122 is important and is observed with the α-carboxylate of DHFR substrate dihydrofolate. The binding of the morpholine oxygen atom with the side chain of Arg122 provides a rigid docking site by restricting the mobility of the flexible linker between the two rings in the designed inhibitors. Several observations have shown that drug molecules designed to occupy the surface volume of the native substrate of the protein will be less susceptible to resistance occurring due to steric clashes in the mutated protein binding site.[41,42]

 This journal is © The Royal Society of Chemistry and the Centre National de la Recherche Scientifique 2014

Published on 11 August 2014. Downloaded by University of Prince Edward Island on 27/10/2014 08:59:50.

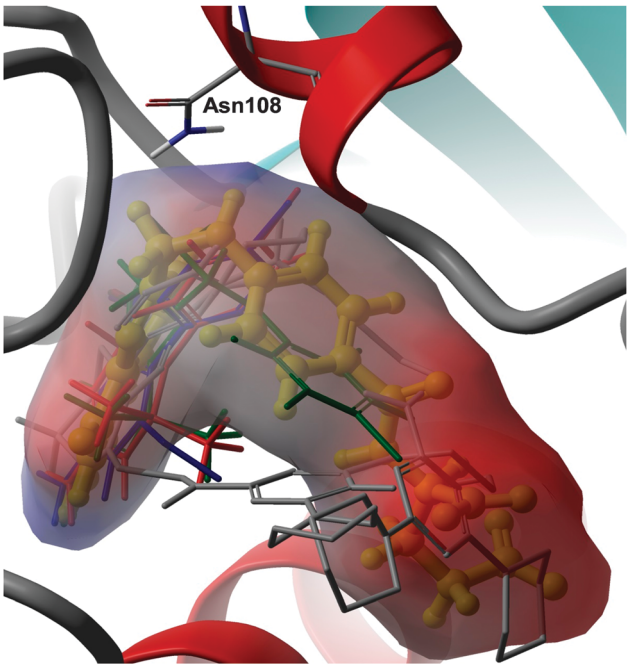

Fig. 5 Superposition of the most active docked test compounds (represented as grey sticks), pyrimethamine (blue sticks), cycloguanil (red sticks), WR99210 (green sticks) and the PfDHFR substrate dihydrofolate (yellow balls and sticks) bound to the binding site of quadruple mutant (PDB ID: 3QG2), showing the fitting of the test compounds on the substrate surface.

Table 3 Prediction of Lipinski's 'Rule of 5' for the active test compounds[a]

Compound	mol_MW	DonorHB	AccptHB	QPlogPo/w	Rule of five
14	472.55	2	12	2.127	1
19	513.64	2	12	2.56	2
25	472.63	2	9	4.532	1
27	471.65	2	9	4.358	1
28	485.68	2	9	4.361	1
30	485.68	2	9	4.728	1
31	499.70	2	9	4.667	1
Pyr	248.71	4	3	1.809	0
Cg	253.73	5	3	0.888	0

[a] All values calculated by QikProp v3.5; the explanations of the descriptors are given in the text. Pyr = pyrimethamine, Cg = cycloguanil.

Thus, it is desirable to explore the binding pattern of the novel lead compound in the preliminary stages of drug design against mutant proteins. The molecular overlay of the docking poses of the active test compounds along with the reference molecules on the dihydrofolate surface envelope clearly shows that the test compounds occupy a similar volume to that of the protein substrate, unlike the dihydrofolate, and avoid steric clash with the side chain of Asn108 (Fig. 5). The results from the present study give us important preliminary information to design novel compounds with a similar scaffold that may lead to more active compounds, which would be a scope for our future communications.

The results of ADMET prediction by QikProp v3.5[43] are presented in Tables 3 and 4. Different pharmacokinetic parameters of the compounds that showed good inhibitory potential in malarial parasites were calculated. The most important of these parameters together with their permissible ranges are listed in Tables 3 and 4.

As a preliminary test of the drug-likeness of the compounds, we calculated Lipinski's rule of 5 using QikProp, which requires compounds to have no more than 5 and 10 hydrogen bond donors (donorHB) and acceptors (accptHB), respectively, molecular weights (mol_MW) of less than 500 amu, and partition coefficients between octanol and water (QPlogP(oct/wat)) of less than 5. Table 3 shows the QikProp results for various parameters of Lipinski's rule of 5. An orally active compound should not have more than one violation of these rules. In the present study, all the active test compounds showed a number of violations of Lipinski's rule of 5 less than the maximum permissible value of 4, indicating that these active test compounds are endowed with drug-like properties. All the compounds showed 1 Lipinski's rule of 5 violation except compound **19**, which showed 2 violations owing to it having mol_MW > 500 and accptHB > 10. Prediction of oral drug absorption (Percent Human Oral Absorption) was highly satisfactory for all the test compounds, with the exception of compound **19**, which showed a moderate value. Studies have suggested that oral bioavailability is influenced by a compound's flexibility and can be measured by the number of rotatable bonds (<15) and the polar surface area (70 Å^2–200 Å^2), though it has been emphasized that this approach should be considered with caution with respect to choice of descriptor algorithm used and also because other factors can have a significant influence on bioavailability.[44] However, along with

Table 4 Calculated ADMET properties

Compound	Percent Human Oral Absorption[a] (>80% high, <25% poor)	QPPCaco[a] nm s^{-1} (<25 poor, >500 great)	QPlogBB[a] (−3.0 to 1.2)	QPPMDCK[a] (<25 poor, >500 great)	QPlogKhsa[a] (−1.5 to 1.5)	QPlogHERG[a] (concern below −5)	QPlogS (−6.5 to 0.5)	PSA[a] (7.0–200.0)	#rotor[a] (0–15)
14	85.123	1899.318	−0.416	989.649	−0.283	−4.251	−3.589	103.834	5
19	61.96	368.938	−0.32	186.276	0.007	−5.674	−3.557	102.564	7
25	100	2146.387	−0.909	1129.502	0.382	−4.903	−4.887	83.75	13
27	87.557	484.098	−0.598	249.85	0.554	−6.464	−5.163	80.387	12
28	88.046	514.064	−0.568	266.608	0.52	−5.977	−4.404	81.384	13
30	90.327	523.024	−0.635	271.635	0.653	−6.588	−5.496	79.854	13
31	89.246	476.685	−0.78	245.718	0.619	−5.988	−4.628	81.492	14
Pyrimethamine	84.346	412.287	−0.78	468.849	−0.243	−4.318	−2.978	73.731	4
Cycloguanil	68.814	111.854	−0.17	126.604	−0.306	−4.578	−1.596	76.262	2

[a] Calculated using QikProp v3.5. Range/recommended values calculated for 95% of known drugs.

Published on 11 August 2014. Downloaded by University of Prince Edward Island on 27/10/2014 08:59:50.

the polar surface area criterion, a total sum of H-bond donors and acceptors criterion (≤ 12) can be used, which is algorithm-independent.[44] In the present study, all the test compounds have a number of rotatable bonds <15 and the polar surface area falls satisfactorily within the permissible range (Table 4). Similarly, molecules obeying Lipinski's rule of 5 could be more likely to have good intestinal absorption or permeation, which is confirmed by the predicted Caco-2 cell permeability (QPPCaco), used as a model for the gut–blood barrier.[45] QPPCaco predictions for all the test compounds showed very good values except for compounds **19**, **27** and **31**, which had moderately good values for Caco-2 cell permeability, comparable to the value predicted for the drug pyrimethamine. Further, QPlogKhsa, the prediction for human serum albumin binding, was carried out for the test compounds and all inhibitors, and the values were within the expected range for 95% of known drugs (−1.5 to 1.5). Also, the QikProp descriptor for the brain/blood partition coefficient (QPlogBB) and the blood–brain barrier mimic MDCK cell permeability (QPPMDCK) show satisfactory predictions for all the test compounds and the reference compounds. In addition, the aqueous solubility (QPlogS) parameter for the test compounds was assessed and all the compounds were predicted to have QPlogS values in the permissible range. Furthermore, the QPlogHERG descriptor for the prediction of the IC_{50} value of HERG K^+ channel blockage was predicted for the test compounds. Compounds **14** and **25** were predicted to possess values in the permissible range comparable to the reference compounds pyrimethamine and cycloguanil (Table 4).

Conclusions

In summary, we report the synthesis, docking studies and evaluation of the antimalarial activity of triazine–pyrimidine molecular hybrids. The *in vitro* evaluation of these hybrids against the D6 and W2 strains of *P. falciparum* revealed activity in the micromolar range, with no cytotoxicity against VERO mammalian cell lines. The active molecules were docked in the active site of wild type and quadruple mutant PfDHFR-TS proteins to study the binding pattern of the test molecules with DHFR. Compounds **14** and **19** were found to show good binding with wild type and mutant DHFR proteins, with an interaction pattern comparable to that of DHFR inhibitors and the native DHFR substrate. Moreover, the test compounds exhibited efficient binding with the mutant protein, avoiding steric clashes resulting from amino acid mutations. The calculated ADMET parameters for the test compounds indicated good pharmacokinetic properties for compound **14**, making it an important candidate in the antimalarial drug discovery process.

Acknowledgements

D.S.R. thanks the Council of Scientific and Industrial Research [No. 02(0049)/12/EMR-II] New Delhi, India for financial support. D.K. is thankful to CSIR for the award of junior and senior research fellowship. P.P. is thankful to CSIR for the award of Research Associate. The United States Department of Agriculture, Agricultural Research Service, Specific Cooperative Agreement No. 58-6408-1-603 is also acknowledged for partial support of this work. The authors are also thankful to CIF-USIC, University of Delhi, Delhi for NMR spectral data, RSIC, CDRI, Lucknow for mass data and Mr John Trott for technical support in antimalarial activity testing at NCNPR.

Notes and references

1 J. Sachs and P. Malaney, *Nature*, 2002, **415**, 680–685.
2 N. J. White, *Lancet*, 2010, **376**, 2051–2052.
3 H. Noedl, Y. Se, K. Schaecher, B. L. Smith, D. Socheat and M. M. Fukuda, *N. Engl. J. Med.*, 2008, **359**, 2619–2620.
4 R. Jambou, E. Legrand, M. Niang, N. Khim, P. Lim, B. Volney, M. T. Ekala, C. Bouchier, P. Esterre, T. Fandeur and O. Mercereau-Puijalon, *Lancet*, 2005, **366**, 1960–1963.
5 A. M. Dondorp, S. Yeung, L. White, C. Nguon, N. P. J. Day, D. Socheat and L. von Seidlein, *Nat. Rev. Microbiol.*, 2010, **8**, 272–280.
6 N. White, *Philos. Trans. R. Soc., B*, 1999, **354**, 739–749.
7 N. Gargano, F. Cenci and Q. Bassat, *Trop. Med. Int. Health*, 2011, **16**, 1466–1473.
8 N. J. White, *Lancet*, 2010, **376**, 2051–2052.
9 H. C. Carrington, A. F. Crowther, D. G. Davey, A. A. Levi and F. L. Rose, *Nature*, 1951, **168**, 1080.
10 N. Alexis, *J. Antimicrob. Chemother.*, 2006, **57**, 1043–1054.
11 A. Gregson and C. V. Plowe, *Pharmacol. Rev.*, 2005, **57**, 117–145.
12 Y. Yuthavong, J. Yuvaniyama, P. Chitnumsub, J. Vanichtanankul, S. Chusacultanachai, B. Tarnchompoo, T. Vilaivan and S. Kamchonwongpaisan, *Parasitology*, 2005, **130**, 249–259.
13 I. M. Kompis, K. Islam and R. L. Then, *Chem. Rev.*, 2005, **105**, 593–620.
14 K. H. Rieckmann, A. E. T. Yeo and M. D. Edstein, *Trans. R. Soc. Trop. Med. Hyg.*, 1996, **90**, 568–571.
15 Y. Yuthavong, T. Vilaivan, S. Kamchonwongpaisan, B. Tarnchompoo, C. Thongpanchang, C. Chitnumsub, J. Yuvaniyama, D. Matthews, W. Charman, S. Charman, L. Vivas and S. B. Katiyar, *US Pat.*, 2009/0099220 A1, 2009.
16 Y. Yuthavong, B. Tarnchompoo, T. Vilaivan, P. Chitnumsub, S. Kamchonwongpaisan, S. A. Charman, D. N. McLennan, K. L. White, L. Vivas, E. Bongard, C. Thongphanchang, S. Taweechai, J. Vanichtanankul, R. Rattanajak, U. Arwon, P. Fantauzzi, J. Yuvaniyama, W. N. Charman and D. Matthews, *Proc. Natl. Acad. Sci. U. S. A.*, 2012, **109**, 16823–16828.
17 M. Delves, D. Plouffe, C. Scheurer, S. Meister, S. Wittlin, E. A. Winzeler, R. E. Sinden and D. Leroy, *PLoS Med.*, 2012, **9**, e1001169.
18 S. B. Katiyar, K. Srivastava, S. K. Puri and P. M. S. Chauhan, *Bioorg. Med. Chem. Lett.*, 2005, **15**, 4957–4960.
19 A. Agarwal, K. Srivastava, S. K. Puri and P. M. S. Chauhan, *Bioorg. Med. Chem. Lett.*, 2005, **15**, 531–533.
20 D. Gravestock, A. L. Rousseau, A. C. U. Lourens, S. S. Moleele, R. L. van Zyl and P. A. Steenkamp, *Eur. J. Med. Chem.*, 2011, **46**, 2022–2030.

 This journal is © The Royal Society of Chemistry and the Centre National de la Recherche Scientifique 2014

Published on 11 August 2014. Downloaded by University of Prince Edward Island on 27/10/2014 08:59:50.

21 J. Morgan, R. Haritakul and P. A. Keller, *Lett. Drug Des. Discovery*, 2008, **5**, 277–280.
22 N. Azas, P. Rathelot, S. Djekou, F. Delmas, A. Gellis, C. Di Giorgio, P. Vanelle and P. Timon-David, *Farmaco*, 2003, **58**, 1263–1270.
23 A. Agarwal, K. Srivastava, S. K. Puri and P. M. S. Chauhan, *Bioorg. Med. Chem. Lett.*, 2005, **15**, 1881–1883.
24 S. Manohar, S. I. Khan and D. S. Rawat, *Bioorg. Med. Chem. Lett.*, 2010, **20**, 322–325.
25 D. S. Rawat, S. Manohar, and U. C. Rajesh, *Indian Pat.*, Application No 661/DEL/2012.
26 S. Manohar, S. I. Khan and D. S. Rawat, *Chem. Biol. Drug Des.*, 2011, **78**, 124–136.
27 S. Manohar, U. C. Rajesh, S. I. Khan, B. L. Tekwani and D. S. Rawat, *ACS Med. Chem. Lett.*, 2012, **3**, 555–559.
28 H. Atheaya, S. I. Khan, R. Mamgain and D. S. Rawat, *Bioorg. Med. Chem. Lett.*, 2008, **18**, 1446–1449.
29 N. Kumar, S. I. Khan, Beena, G. Rajalakshmi, P. Kumaradhas and D. S. Rawat, *Bioorg. Med. Chem*, 2009, **17**, 5632–5638.
30 N. Kumar, S. I. Khan, H. Atheaya, R. Mamgain and D. S. Rawat, *Eur. J. Med. Chem.*, 2011, **46**, 2816–2827.
31 J. Singh, R. K. S. Dhakarey, S. V. Singh, M. K. Suthar, J. K. Saxena and A. K. Dwivedi, *Chem. Biol. Interface*, 2012, **2**, 347–361.
32 K. Doktorov, V. B. Kurteva, D. Ivanova and I. Timtcheva, *ARKIVOC*, 2007, **15**, 232–245.
33 V. B. Kurteva and C. A. M. Afonso, *Green Chem.*, 2004, **6**, 183–187.
34 N. Kumar, S. I. Khan and D. S. Rawat, *Helv. Chim. Acta*, 2012, **95**, 1181–1197.
35 M. Jain, S. I. Khan, B. L. Tekwani, M. R. Jacob, S. Singh, P. P. Singh and R. Jain, *Bioorg. Med. Chem.*, 2005, **13**, 4458–4466.
36 M. T. Makler and D. J. Hinrichs, *Am. J. Trop. Med. Hyg.*, 1993, **48**, 205–210.
37 J. Mustafa, S. I. Khan, G. Ma, L. A. Walker and I. A. Khan, *Lipids*, 2004, **39**, 167–171.
38 D. S. Peterson, W. K. Milhous and T. E. Wellems, *Proc. Natl. Acad. Sci. U. S. A.*, 1990, **87**, 3018–3022.
39 E. M. Duffy and W. L. Jorgensen, *J. Am. Chem. Soc.*, 2000, **122**, 2878–2888.
40 J. Yuvaniyama, P. Chitnumsub, S. Kamchonwongpaisan, J. Vanichtanankul, W. Sirawaraporn, P. Taylor, M. D. Walkinshaw and Y. Yuthavong, *Nat. Struct. Biol.*, 2003, **10**, 357–365.
41 N. M. King, M. Prabu-Jeyabalan, E. A. Nalivaika and C. A. Schiffer, *Chem. Biol.*, 2004, **11**, 1333–1338.
42 K. P. Romano, A. Ali, W. E. Royer and C. A. Schiffer, *Proc. Natl. Acad. Sci. U. S. A.*, 2010, **107**, 20986–20991.
43 QikProp User Manual Copyright © 2013 Schrödinger, LLC.
44 J. J. Lu, K. Crimin, J. T. Goodwin, P. Crivori, C. Orrenius, L. Xing, P. J. Tandler, T. J. Vidmar, B. M. Amore, A. G. E. Wilson, P. F. W. Stouten and P. S. Burton, *J. Med. Chem.*, 2004, **47**, 6104–6107.
45 P. Artursson, K. Palm and K. Luthman, *Adv. Drug Delivery Rev.*, 2001, **46**, 27–43.